Hindawi
Journal of Chemistry
Volume 2022, Article ID 9944126, 8 pages
https://doi.org/10.1155/2022/9944126

Research Article

Effective Removal of Phosphate from Waste Water Based on Silica Nanoparticles

Tan Tai Nguyen

Department of Materials Science, School of Applied Chemistry, Tra Vinh University, Tra Vinh 87000, Vietnam

Correspondence should be addressed to Tan Tai Nguyen; nttai60@tvu.edu.vn

Received 13 August 2022; Revised 30 October 2022; Accepted 2 November 2022; Published 14 November 2022

Academic Editor: Doina Humelnicu

This study explored the potential application of silica nanoparticles (SiNPs) prepared from rice husk ash (RHA) to reuse phosphate from aqueous solution. The physicochemical analysis illustrated that the SiNPs, which were extracted from waste biomass, have a nonuniform shape with a size range of a few nanometer to hundreds of nanometers, a surface area of 15.56 $m^2 \cdot g^{-1}$, and an adsorption pore width of 4.06 nm. Those results carried out the possibility to utilize the SiNPs for removal of phosphate. Findings from the batch sorption experiments showed that the phosphate adsorption was controlled by experimental parameters, i.e., pH, adsorbent dosage, concentration of adsorbate, and adsorption time. The experimental results showed that the maximum phosphate adsorption capacity of SiNPs was achieved at around 9.08 $mg \cdot g^{-1}$ at adsorption conditions, i.e., pH 7, SiNPs dosage of 0.3 g, and adsorption time of 90 min. The phosphate removal based on SiNPs will offer several benefit such as an effective and low cost method, reliable to reuse as an effective slow release phosphate fertilizer.

1. Introduction

Nowadays, using a lot of fertilizer has caused the release of nutrients, such as phosphorus and nitrogen, from agriculture and aquaculture fields to aquatic systems [1–3]. Leaching of nutrients may lead to many problems such as acceleration of soil acidification and especially to the environmental health [4, 5]. An increase in the amount of phosphate may be associated with the increment of aquatic organism that caused water eutrophication [3, 6–8]. An option to remove phosphate leaching has been reported including biological, chemical, and physical treatment methods such as bioreactor system [9, 10], electrochemical reaction [11, 12], electrodialysis [13, 14], wetland treatment system [15, 16], and anion exchange ion [17–21]. In addition, many physical techniques have been developed to remove phosphate from aqueous solution such as reverse osmosis, ion exchange, electrodialysis, and adsorption. Among these, physical adsorption methods have been studied and widely used for the removal of phosphate ions due to their benefits, i.e., high capacity of adsorption, ease-of-use, low cost, and environmental friendly methods [22–25]. In addition, several promising materials have been used for phosphate removal such as red mud [26], calcium carbonate [27], activated alumina [28], calcium kaolinite [29], soil, fly ash, and coal slag [30–32]. However, these methods have inherent drawbacks such as difficult to maintain biological process at optimum condition, being complicated in operation, high cost, and time-consuming methods. Moreover, these materials required pretreatment for the removal process. It is worth to mention that silica nanoparticles (SiNPs) are promising materials for the removal of phosphate with its high adsorption capacity. Vietnam, the second largest producer of rice in the world, produces about 43.86 billion kilogram a year. In addition, the rice husk ash (RHA), which is contained high amount of silica (approximately 90%), is by-product of a brick-kiln industry. So, the reuse and recycling process of RHA for extraction of SiNPs is cost-effective and environmental friendly method.

The object of the present study was to evaluate the potential of SiNPs extracted from rice husk ash for phosphate removal from an aqueous solution. The physicochemical property of the SiNPs was investigated, and the adsorption conditions were optimized based on several

factors including pH, adsorbent dosage, contact time, and concentration of adsorbate. Adsorption isotherms were also studied at different concentration of phosphate.

2. Materials and Methods

2.1. Reagents. The rice husk ash was taken from brick-kiln industry (Tra Vinh Province, Vietnam). Chemical agents including sodium hydroxide (NaOH), sulfuric acid (H_2SO_4, 98%), hydrochloric (HCl, 98%), potassium phosphate monobasic (KH_2PO_4, 99%), potassium antimony tartrate hemidydrate ($K(SbO)C_4H_4O_6$ $1/2H_2O$, 99.5%), acid ascorbic ($C_8H_8O_6$, 99%), and ammonium molybdate tetrahydrate ($(NH_4)_6Mo_7O_{24}.4H_2O$, 99.98%) were purchased from Sigma-Aldrich.

2.2. Preparation of SiO_2 Nanoparticles. SiO_2 NPs were synthesis based on RHA with sol-gel method. The extraction process has been studied and found in the literature [33]. In this work, this could be briefly described with four steps as illustrated in Figure 1. For the first step, RHA (2 g) was taken from brick-kiln industry and washed three times for removing dirt under DI water (Figure 1(a)). Then, the sodium silicate was generated by using collected RHA that was put in the NaOH solution (v/v concentration of 3.5 M) with the stirring speed of 400 rpm. The mixture was then filtrated to carry off the nonreactive impurities (Figure 1(b)). The concentration of 4 M (HCl) was added to the obtained sodium silicate solution under vigorous stirring in order to initiate the hydrolysis-condensation reaction at pH~7 (Figure 1(c)). The obtained gel was dispersed in ethanol and washed three times with DI water. Then, the gel was dried at 110°C for 2 h. The synthesized SiO_2 NPs was stored in desiccator for future use.

2.3. Adsorption Process for the Removal of Phosphate. In this work, the phosphate adsorption capacity of SiNPs was studied with various factors at room temperature. The concentration of phosphate was set from 0.5 to 2.5 $mg{\cdot}L^{-1}$ and was measured by stannous chloride method, monitoring the absorbance at 690 nm on UV-Vis spectrometer [31]. The effect of pH was investigated in the range 5–9 by controlling the pH of phosphate solution utilizing NaOH and HCl solutions and was measured utilizing pH meter (pH Meter 7110 SET, WTW). The contact time was changed from 30 to 150 min. The effect of adsorbent dosage was studied with different adsorbent doses from 0.1 to 0.5 g with an increment of 0.1 g. The adsorption experiments were carried out with a stirring speed of 200 rpm at room temperature. The phosphate adsorption capacity (q_{AC}) was estimated by using the equation below [30]:

$$q_{AC} = \frac{C_{in} - C_{fn}}{m_{SiNPs}}, \quad (1)$$

where C_{in} is the concentration of phosphate ion at the initial state, C_{fn} is the concentration of phosphate ions at the equilibrium state, m_{SiNPs} is adsorbent's mass, and V is the adsorbate's volume.

2.4. Physicochemical and Morphological Characterization. The physicochemical characterization of SiNPs and adsorption of phosphate ions was obtained based on several analytical techniques: Transmission Electron Microscopy (TEM, Keyence VKX-1000) for ultrastructural analysis; Fourier Transform Infrared Spectroscopy (FTIR, Thermo Scientific Nicolet iS50) for determination of functional groups in a range 4000–500 cm^{-1}; Energy Dispersive *X*-ray Spectroscopy (EDS) for the elemental composition of SiO_2 extracted; Ultraviolet-Visible Spectroscopy (UV-Vis, Shimazu UV-2600) for measurement of concentration of phosphate solution; pore size distribution obtained by BJH (Micrometrics ASAP 2010); surface area measured by the BET method.

3. Results and Discussion

3.1. Characterization of SiNPs. In this work, SiNPs were extracted from rice husk and physicochemical properties were then analyzed by the Transmission Electronic Microscopy (TEM) for ultrastructural analysis, the Fourier Transform Infrared Spectroscopy (FTIR) for determination of functional groups in a range of 500–4000 cm^{-1}, and Energy Dispersive *X*-ray Spectroscopy (EDS) for composition analysis. Pore size distribution obtained by BJH and surface are measured by the BET method. The results of FTIR analysis represented that the adsorption peaks were achieved at 794 cm^{-1}, 956 cm^{-1}, and 1069 cm^{-1}, which are due to the asymmetric, symmetric, and bending modes of SiNPs, respectively, as shown in Figure 2(a). A TEM micrograph of SiNPs (Figure 2(b)) illustrated that the formed SiNPs were aggregated and the size ranged from a few nanometers to several hundred nanometers. In addition, analyzing the curves in Table 1 can carry out some light on the purities of SiO_2 extracted. The SiNPs extracted contained Si and O, which are compositions of 28.22 and 50.82%, respectively. The remaining of impurities (Na, Cl, Al, and K) was due to unperfect washing process. Moreover, BET and BJH analysis showed that SiNPs proposed a specific surface area of 15.56 $m^2{\cdot}g^{-1}$ with an average pore size of 4.06 nm, leading to provide potential materials for removal of phosphate.

3.2. Effect of Initial Solution pH. To investigate the adsorption behavior of a phosphate ion, all adsorption experiments were performed based on batchwise method to investigate the influence of pH, adsorbent mass, and contact time. Experiments to study the effect of pH were carried out as follows: 0.2 g of adsorbent was added to 50 cm^3 of 2 $mg{\cdot}L^{-1}$ aqueous sodium phosphate solution, and then the mixture solution was stirred at a speed of 200 rpm at 300 K. It should be noted that each data point in Figures 3 and 4 are represented by the mean value of three experimental results. As shown in Figure 3, the phosphate adsorption capacity was associated with pH value. When pH increased, the adsorption capacity increased. The maximum value was achieved around 4.8 $mg{\cdot}g^{-1}$ at pH 7. The phosphate adsorption capacity was dropped down when pH value was

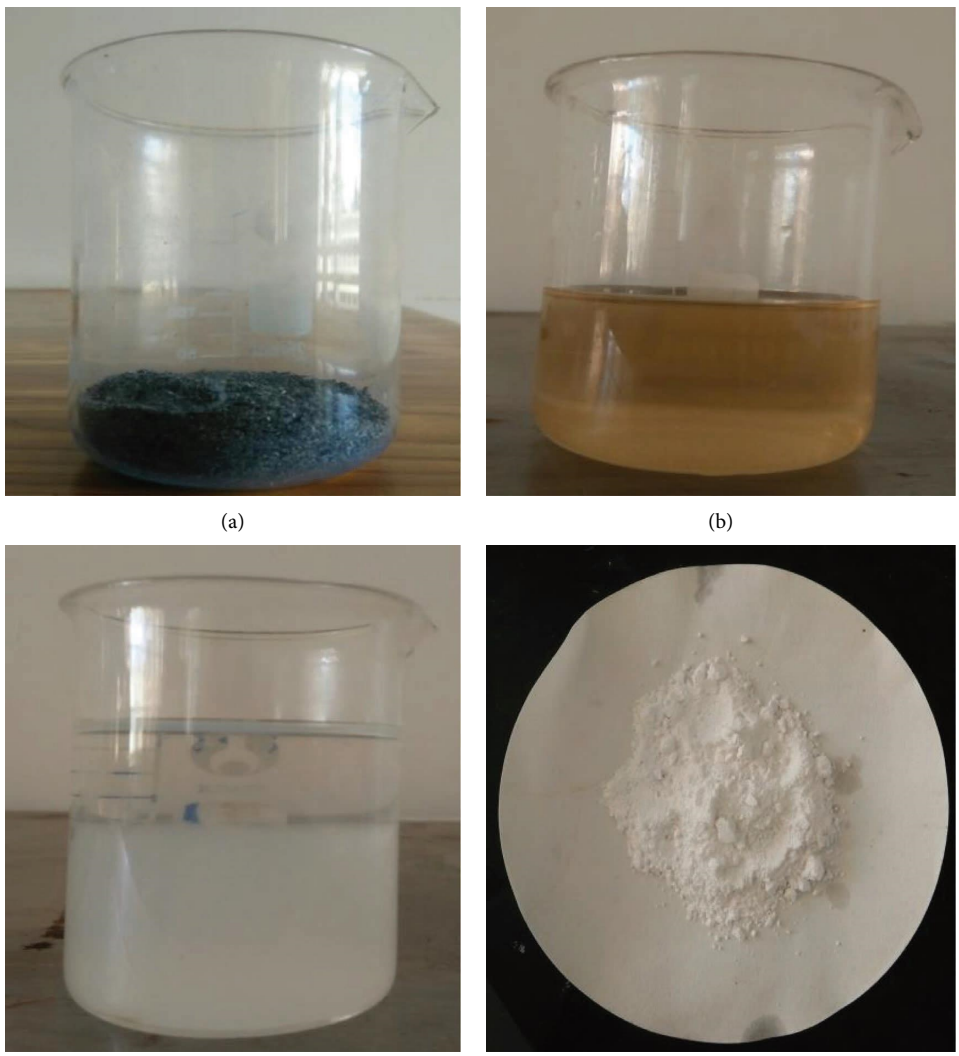

(a) (b)

(c) (d)

Figure 1: The SiO_2 extraction process. *Note.* (a) Rice husk ash; (b) filtering solution from rice husk ash diluted in sodium hydroxide; (c) precipitation by acid; (d) SiO_2 powder.

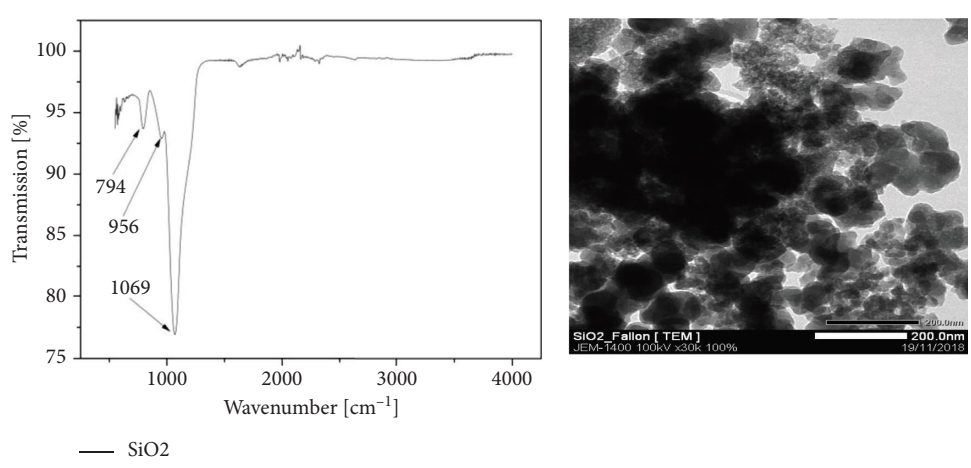

(a) (b)

Figure 2: SiNPs characterization. Fourier transform infrared spectrum (a); TEM image (b).

Table 1: Energy dispersive *X*-ray spectroscopy analysis of SiNPs.

Elements	Si	O	Na	Cl	Al	K
% Weight	28.22	50.82	8.63	8.04	3.09	1.19

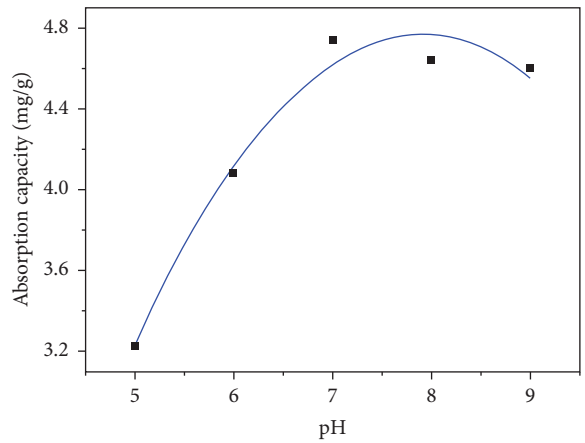

Figure 3: Influence of pH to the adsorption capacity of phosphate.

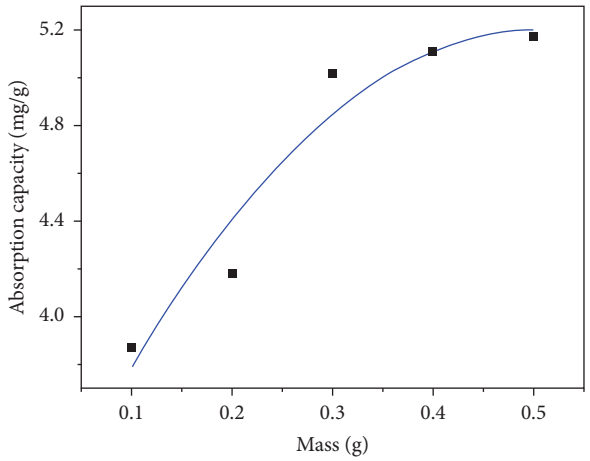

Figure 4: Influence of mass of SiNPs to the adsorption capacity of phosphate.

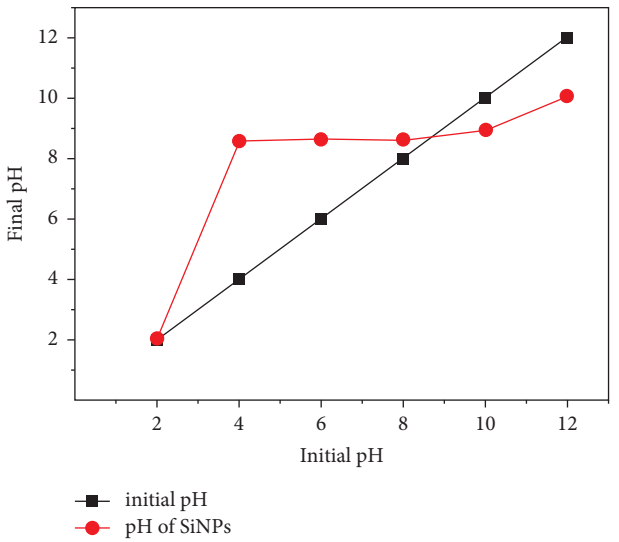

Figure 5: The pHpzc determination curve of the SiNPs.

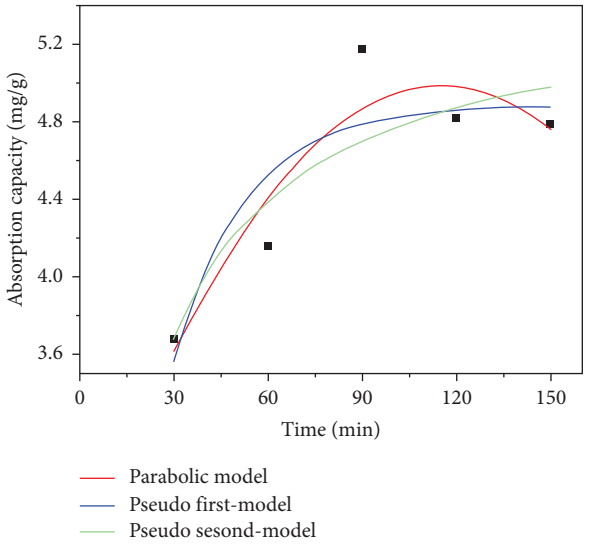

Figure 6: Adsorption kinetics of phosphate ions by SiNPs.

lower or higher than 7. The adsorption phenomena could be explained based on the surface charge of SiNPs. In this case, the experiments were conducted to measure the pH at the potential of zero point charge (pHpzc) based on the pH drift method as shown in Figure 5. The initial pH was set in the pH range of 2 to 12 with an increment of 2 pH unit. Then, the SiNPs of 100 mg was added into the solution for 24 h at a stirring speed of 200 rpm. The experimental results showed that the pHpzc of SiNPS obtained was around 8.7. The SiNPs has a negative surface charge at pH < 7 and positive surface charge at pH > 8. The adsorption behavior of SiNPs surface could be explained based on the competition of three different charges, i.e., H^+, OH^-, and PO_4^{3-} of the surrounding medium at pH < 7 or at pH > 8. This indicates that phosphate ions were physically adsorbed on the surface of SiNPs through the pore capillaries at the optimizing 7 < pH < 8.7, which corresponds to pHpzc of SiNPs. The pH increased or decreased, the salinity may prevent phosphate adsorption by Al oxide by making deformation of phosphate from $H_2PO_4^-$ to HPO_4^{2-} and by a change to the surface charge of the oxide mentioned [34].

3.3. Effect of SiNPs Dosage. In this work, the parabolic shape curve with a quadratic second order equation $q = q_o + ax + bx^2$ was used to fit to the experimental data presented in Figures 3, 4, and 6 [30]. This is to find an ideal characteristic shape for removing phosphate with various parameters, i.e., pH, mass, and contact time. The analysized results showed that the minimum adsorption capacity of phosphate (q_o) based on SiNPs was 0.8 mg·g^{-1} for pH change (Figure 3), 4.98 mg·g^{-1} for SiNPs dosage change (Figure 4), and 4.47 mg·g^{-1} for adsorption time change (Figure 6), respectively. The fitting results also illustrated that, in the

Table 2: Kinetic coefficients for removing phosphate.

	Minimum capacity of adsorption q_o (mg·g^{-1})	Fitting parameters		
		a (a.u.)	b (a.u.)	R^2
Time	4.47	0.04	−1.89	0.74
Mass	4.98	8.89	−8.93	0.88
pH	0.8	2.87	−0.18	0.96

Table 3: Adsorption coefficients for kinetic models.

	Possible adsorption capacity q_{ad} (mg·g^{-1})	Kinetic coefficients		
		P_1 (min^{-1})	P_2 (g·mg^{-1}·min^{-1})	R^2
Pseudo-first-order model	4.89	0.04	—	0.55
Pseudo-second-order model	5.46	—	0.01	0.92

case of pH, the minimum possible adsorption capacity drops to a value 6 times lower than in the other cases. This was caused by the deformation of phosphate ion from $H_2PO_4^-$ to HPO_4^{2-}, SiNPs surface charge, as discussed above. In addition, all of the correlation coefficients (R^2) for three different cases including effect of pH, effect of mass, and change of adsorption time were higher than 0.70 as shown in Table 2. This indicated that the model proposed, i.e., the quadratic second order equation, fitted well into the experimental data.

3.4. Adsorption Isotherm and Their Modelling. Furthermore, Figure 6 represents the adsorption kinetics of SiNPs extracted. The figure showed the adsorption capacity of 5.2 mg·g^{-1} with the optimized conditions, i.e., adsorption time of 90 min with a SiNPs loading mass of 0.3 g. Figure 6 shows that, the phosphate ions were slowly adsorbed by SiNPs and achieved a plateau value at 90 min. Moreover, the initial adsorption rate of 0.12 mg·g^{-1}·min^{-1} was achieved based on the experimental data. It is worth mentioning that the lower the adsorption rate is, the shorter the plateau time is. This relatively low adsorption rate of SiNPs can be contributed to the weak diffusion of phosphate ions from surface adsorption sites to the bulk SiNPs pore, which is mainly caused by the small pore size of 4.06 nm. In addition, the adsorption kinetics was investigated by utilizing the pseudo-first-order kinetic model (Equation (2)) and the pseudo-second-order kinetic model (Equation (3)) as given below [35, 36]:

$$q_t = q_{ad}\left(1 - e^{-P_1 t}\right), \tag{2}$$

$$q_t = \frac{t}{\left(1/P_2 q_{ad}^2\right) + \left(t/q_{ad}\right)}, \tag{3}$$

where q_{ad} and q_t were the adsorption capacities of phosphate at the plateau time and t, respectively. P_1 and P_2 were the pseudo-first- and the pseudo-second-order rate constants, respectively. It should be noted that the first pseudo kinetic model and the second ones represented the kinetic adsorption of mononuclear and binuclear of the solid-liquid system, respectively. Table 3 presents the adsorption coefficients that were achieved based on those above equations. In addition, Figure 6 presented a comparison between the parabolic model and the two pseudo kinetic models. The phosphate adsorption capacity was estimated around 5.0 mg·g^{-1} as presented in Table 3. This value agrees with the experimental results. Moreover, the correlation coefficient (R^2) was obtained around 0.74; 0.55; 0.92 for the case of the parabolic model, the pseudo-first-kinetic model, and the pseudo-second-kinetic model, respectively. These results indicated that the phosphate adsorption system studied belongs to the pseudo-second-kinetic model.

The models of adsorption isotherm are important for the prediction of the adsorption process to design the adsorption system. Normally, the adsorption capacity could be estimated based on choosing the approximate dosage of adsorbent. In this work, the phosphate concentration was set in the range of 0.5 to 2.5 mg·L^{-1}. Then, the experiment was performed based on the optimum parameters, i.e., pH 7, SiNPs dosage of 0.3 g, and adsorption time of 90 min at room temperature. Then, the Langmuir (Equation (4)) and Freundlich (Equation (5)) models were applied to analyze the experimental data, respectively [35, 37].

$$C_{\text{eq}} = \frac{q_{eq}}{A_L\left(q_{\max} - q_{eq}\right)}, \tag{4}$$

$$\log q_{eq} = I \log C_{eq} + \log A_F, \tag{5}$$

where C_{eq}, q_{eq}, and $q_{\max}$ were the phosphate concentration, the adsorption capacity of phosphate at the equilibrium state, and the maximum adsorption capacity of phosphate, respectively; A_L was the adsorption energy; I was the adsorption intensity; A_F was the adsorption affinity.

The fitting parameters, i.e., the adsorption factors and the correlation coefficients, were obtained based on the Langmuir (Figure 7(a)) and Freundlich (Figure 7(b)) models as illustrated in Table 4. The adsorption intensity (I) of 0.34, which was estimated utilizing the Freundlich model, was smaller than one that represented a low adsorption rate of the phosphate ions. This leads to the long adsorption time of 90 min as mentioned in Figure 6. In Table 4, the affinity between adsorbent and phosphate ions was estimated at around 0.69 mg·g^{-1} offered weak interaction between SiNPs

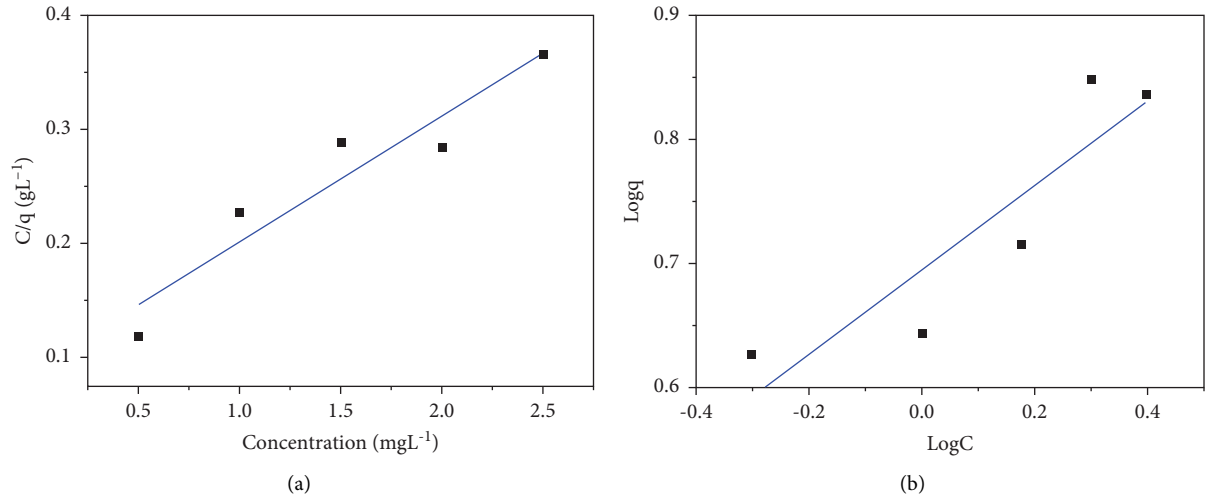

Figure 7: Langmuir isotherm model (a) and Freundlich isotherm model (b) for removing phosphate by SiNPs.

Table 4: Adsorption isotherm parameters removal of phosphate.

	Maximum adsorption capacity q_{max} (mg·g^{-1})	Isotherm coefficients			
		A_F (mg·g^{-1})	I	A_L (L·mg^{-1})	R^2
Freundlich isotherm	—	0.69	0.34	—	0.75
Langmuir isotherm	9.08	—	—	1.2	0.87

Table 5: Comparison of phosphate ion adsorption between SiO_2 and another materials.

Materials	Concentration range (mg·L^{-1})	Adsorption capacity (mg·g^{-1})	Treatment	Reference
SiO_2	0.5–2.5	9.08	Without treatment	This study
Fly ash	50–2000	3.34	Without treatment	[38]
Steel slag	11.40–45.59	5.30	Without treatment	[39]
Red mud	0.01–1	0.58	HCl treatment, pH = 5, 40°C	[26]

surface and phosphate ions. It should be noted that the lager A_L values produced the higher adsorption of phosphate in an approximately linear fashion. This result was given agreement with the low initial adsorption rate of 0.12 mg·g^{-1}·min^{-1} as mentioned above. Unlike the Freundlich isotherm model, the Langmuir isotherm model was a practical model which proposed a maximum adsorption capacity of the phosphate. In Figure 7(b), the Langmuir isotherm model exhibited a maximum adsorption capacity of 9.08 mg·g^{-1}, which is higher compared to the research found in the literature as depicted in Table 5. In addition, the Langmuir isotherm described a better fit using the experimental data based on correlation coefficient (R^2), which was higher than that of Freundlich isotherm. This leads us to believe that SiNPs can be applied to remove phosphate from waste water as an effective method.

3.5. Comparison of SiNPs with Other Absorbents. Table 5 presents the phosphate ion adsorption of SiNPs and other materials including fly ash, steel slag, and red mud. It can be absorved that the maximum adsorption capacity of SiNPs is better than that of other adsorbents under similar experimental condition. Therefore, the use of SiNPs for the adsorption of phosphate is a friendly and cost-effective method. In addition, the use of SiNPs may offer several benefits for the adsorption of heavy metals based on conjugation with various functional groups for specific detection such as heavy metal ions (Pb^{2+}, Cu^{2+}, Cr^{6+}), for environmental applications.

4. Conclusions

In conclusion, this study investigated the ability of SiNPs extracted from rice husk ash to adsorb phosphate from aqueous solution under various parameters, i.e., mass of adsorbent, pH, adsorbate concentration, and adsorption time. The experimental results showed that the maximum adsorption capacity of 9.08 mg SiNPs g^{-1} phosphate was obtained at pH 7, SiNPs dosage of 0.3 g, and adsorption time of 90 min. The phosphate adsorption capacity can be enhanced by the surface modification of the SiNPs with functional groups. In addition, the use of SiNPs for removing phosphate ions not only offers an ease-of-use method and high efficient but also low cost of adsorbents.

Data Availability

This data used to support the findings of this study are available from the corresponding author upon request.

Conflicts of Interest

The authors declare that they have no conflicts of interest.

Acknowledgments

This research was supported by Tra Vinh University under Basic Science Research.

References

[1] H. Ackefors and M. Enell, "Discharge of nutrients from Swedish fish farming to adjacent sea areas," *Ambio*, vol. 19, no. 1, pp. 28–35, 1990.

[2] S. R. Carpenter, N. F. Caraco, D. L. Correll, R. W. Howarth, A. N. Sharpley, and V. H. Smith, "Nonpoint pollution of surface waters with phosphorus and nitrogen," *Ecological Applications*, vol. 8, no. 3, pp. 559–568, 1998.

[3] J. Seppälä, S. Knuuttila, and K. Silvo, "Eutrophication of aquatic ecosystems a new method for calculating the potential contributions of nitrogen and phosphorus," *International Journal of Life Cycle Assessment*, vol. 9, no. 2, pp. 90–100, 2004.

[4] H. Ackefors and M. Enell, "The release of nutrients and organic matter from aquaculture systems in Nordic countries," *Journal of Applied Ichthyology*, vol. 10, no. 4, pp. 225–241, 1994.

[5] K. K. Vass, A. Wangeneo, S. Samanta, S. Adhikari, and M. Muralidhar, "Phosphorus dynamics, eutrophication and fisheries in the aquatic ecosystems in India," *Current Science*, vol. 108, no. 7, pp. 1306–1314, 2015.

[6] J. Van Rijn, "Waste treatment in recirculating aquaculture systems," *Aquacultural Engineering*, vol. 53, pp. 49–56, 2013.

[7] D. Bulgariu, O. Axinte, I. S. Badescu, C. Stroe, V. Neacsu, and L. Bulgariu, "Evolution of trophic parameters from Amara lake," *Environmental Engineering and Management Journal*, vol. 14, no. 3, pp. 559–565, 2015.

[8] A. L. Gentelini, J. H. Oxford, A. C. Godoy et al., "The influence of aquaculture on the hydro-geochemistry of a neotropical aquatic system," *Aquaculture*, vol. 533, Article ID 736179, 2021.

[9] E. Bock, N. Smith, M. Rogers et al., "Enhanced nitrate and phosphate removal in a denitrifying bioreactor with biochar," *Journal of Environmental Quality*, vol. 44, no. 2, pp. 605–613, 2015.

[10] G. Hua, M. W. Salo, C. G. Schmit, and C. H. Hay, "Nitrate and phosphate removal from agricultural subsurface drainage using laboratory woodchip bioreactors and recycled steel byproduct filters," *Water Research*, vol. 102, pp. 180–189, 2016.

[11] E. Lacasa, P. Canizares, C. Saez, F. J. Fernandez, and M. A. Rodrigo, "Electrochemical phosphates removal using iron and aluminium electrodes," *Chemical Engineering Journal*, vol. 172, no. 1, pp. 137–143, 2011.

[12] S. Pulkka, M. Martikainen, A. Bhatnagar, and M. Sillanpää, "Electrochemical methods for the removal of anionic contaminants from water-a review," *Separation and Purification Technology*, vol. 132, no. 20, pp. 252–271, 2014.

[13] Y. Zhang, E. Desmidt, A. Van Looveren, L. Pinoy, B. Meesschaert, and B. Van der Bruggen, "Phosphate separation and recovery from wastewater by novel electrodialysis," *Environmental Science & Technology*, vol. 47, no. 11, pp. 5888–5895, 2013.

[14] K. C. Kedwell, M. K. Jørgensen, C. A. Quist-Jensen, T. D. Pham, B. Van der Bruggen, and M. L. Christensen, "Selective electrodialysis for simultaneous but separate phosphate and ammonium recovery," *Environmental Technology*, vol. 42, no. 14, pp. 2177–2186, 2021.

[15] Z. Wang, J. Dong, L. Liu, G. Zhu, and C. Liu, "Screening of phosphate-removing substrates for use in constructed wetlands treating swine wastewater," *Ecological Engineering*, vol. 54, pp. 57–65, 2013.

[16] S. Nandakumar, H. Pipil, S. Ray, and A. K. Haritash, "Removal of phosphorous and nitrogen from wastewater in brachiaria-based constructed wetland," *Chemosphere*, vol. 233, pp. 216–222, 2019.

[17] L. M. Blaney, S. Cinar, and A. K. SenGupta, "Hybrid anion exchanger for trace phosphate removal from water and wastewater," *Water Research*, vol. 41, no. 7, pp. 1603–1613, 2007.

[18] N. Y. Acelas, B. D. Martin, D. López, and B. Jefferson, "Selective removal of phosphate from wastewater using hydrated metal oxides dispersed within anionic exchange media," *Chemosphere*, vol. 119, pp. 1353–1360, 2015.

[19] N. C. Lu and J. C. Liu, "Removal of phosphate and fluoride from wastewater by a hybrid precipitation–microfiltration process," *Separation and Purification Technology*, vol. 74, no. 3, pp. 329–335, 2010.

[20] S. Yagi and K. Fukushi, "Removal of phosphate from solution by adsorption and precipitation of calcium phosphate onto monohydrocalcite," *Journal of Colloid and Interface Science*, vol. 384, no. 1, pp. 128–136, 2012.

[21] Y. Wang, P. Kuntke, M. Saakes, R. D. van der Weijden, C. J. Buisman, and Y. Lei, "Electrochemically mediated precipitation of phosphate minerals for phosphorus removal and recovery: progress and perspective," *Water Research*, vol. 209, Article ID 117891, 2022.

[22] A. El Midaoui, F. Elhannouni, M. Taky et al., "Optimization of nitrate removal operation from ground water by electrodialysis," *Separation and Purification Technology*, vol. 29, no. 3, pp. 235–244, 2002.

[23] A. Kapoor and T. Viraraghavan, "Nitrate removal from drinking water—review," *Journal of Environmental Engineering*, vol. 123, no. 4, pp. 371–380, 1997.

[24] F. Lutin and G. Guerif, *Electrodialysis Applied to Denitration of Drinking Water*, Water Treatment and Pervaporation, vol. 189, pp. 200–208, 1982.

[25] R. Rautenbach, W. Kopp, R. Hellekes, R. Peter, and G. Vanopbergen, "Separation of nitrate from well water by membrane processes (reverse osmosis/electrodialysis reversal)," *Aqua*, vol. 5, pp. 279–282, 1986.

[26] W. Huang, S. Wang, Z. Zhu et al., "Phosphate removal from wastewater using red mud," *Journal of Hazardous Materials*, vol. 158, no. 1, pp. 35–42, 2008.

[27] H. Arslanoğlu, "Production of low-cost adsorbent with small particle size from calcium carbonate rich residue carbonatation cake and their high performance phosphate adsorption applications," *Journal of Materials Research and Technology*, vol. 11, pp. 428–447, 2021.

[28] E. Szatyłowicz and I. Skoczko, "Studies on the efficiency of groundwater treatment process with adsorption on activated alumina," *Journal of Ecological Engineering*, vol. 18, no. 4, pp. 211–218, 2017.

[29] Y. Li, B. Xia, Q. Zhao et al., "Removal of copper ions from aqueous solution by calcium alginate immobilized kaolin," *Journal of Environmental Sciences*, vol. 23, no. 3, pp. 404–411, 2011.

[30] P. Pengthamkeerati, T. Satapanajaru, and P. Chularuengoaksorn, "Chemical modification of coal fly ash for the removal of phosphate from aqueous solution," *Fuel*, vol. 87, no. 12, pp. 2469–2476, 2008.

[31] N. Hoang Lam, H. T. Ma, M. J. K. Bashir, G. Eppe, P. Avti, and T. T. Nguyen, "Removal of phosphate from wastewater using coal slag," *International Journal of Environmental Analytical Chemistry*, vol. 101, no. 15, pp. 2668–2678, 2021.

[32] S. H. Hong, A. M. Ndingwan, S. C. Yoo, C. G. Lee, and S. J. Park, "Use of calcined sepiolite in removing phosphate from water and returning phosphate to soil as phosphorus fertilizer," *Journal of Environmental Management*, vol. 270, Article ID 110817, 2020.

[33] T. T. Nguyen, H. T. Ma, P. Avti et al., "Adsorptive removal of iron using SiO_2 nanoparticles extracted from rice husk ash," *Journal of Analytical Methods in Chemistry*, vol. 2019, Article ID 6210240, 8 pages, 2019.

[34] P. Ning, H. J. Bart, B. Li, X. Lu, and Y. Zhang, "Phosphate removal from wastewater by model-La (III) zeolite adsorbents," *Journal of Environmental Sciences*, vol. 20, no. 6, pp. 670–674, 2008.

[35] P. K. To, H. T. Ma, L. Nguyen Hoang, and T. T. Nguyen, "Nitrate removal from waste-water using silica nanoparticles," *Journal of Chemistry*, vol. 2020, Article ID 8861423, 6 pages, 2020.

[36] D. Panias, I. P. Giannopoulou, and T. Perraki, "Effect of synthesis parameters on the mechanical properties of fly ash-based geopolymers," *Colloids and Surfaces A: Physicochemical and Engineering Aspects*, vol. 301, no. 1–3, pp. 246–254, 2007.

[37] M. Šešlija, A. Rosić, N. Radović, M. Vasić, M. Đogo, and M. Jotić, "Properties of fly ash and slag from power plants," *Geologia Croatica*, vol. 69, no. 3, pp. 317–324, 2016.

[38] S. G. Lu, S. Q. Bai, L. Zhu, and H. D. Shan, "Removal mechanism of phosphate from aqueous solution by fly ash," *Journal of Hazardous Materials*, vol. 161, no. 1, pp. 95–101, 2009.

[39] J. Yu, W. Liang, L. Wang, F. Li, Y. Zou, and H. Wang, "Phosphate removal from domestic wastewater using thermally modified steel slag," *Journal of Environmental Sciences*, vol. 31, pp. 81–88, 2015.